**Supporting Information**

# Fluorescence Turn-off Mechanism of Norbornene Derived Homopolymer – An $Al^{3+}$ Colorimetric and Fluorescent Chemosensor

*Trong-Nghia Le,†, Kuan-Yu Lin,† Anusha Valaboju, Cheng-Kang Lee, Jyh-Chiang Jiang* and N.Vijayakameswara Rao**
Department of Chemical Engineering, National Taiwan University of Science and Technology, Taipei, Taiwan.
† These authors contributed equally to this work.
*Corresponding author:
**Jyh-Chiang Jiang**, e-mail: jcjiang@mail.ntust.edu.tw
**Vijayakameswara Rao**, e-mail: vijayrao@mail.ntust.edu.tw

## List of Figures



## List of Tables

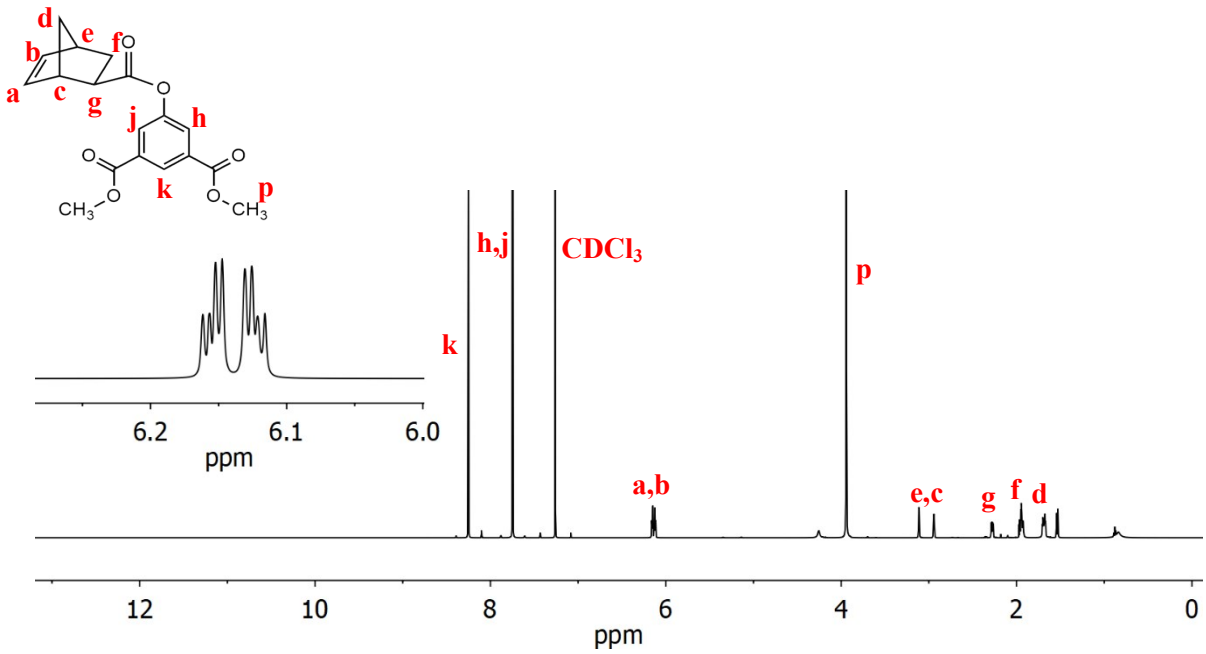


**Figure S1.** $^{1}$H NMR spectra of NDMIP in $CDCl_3$

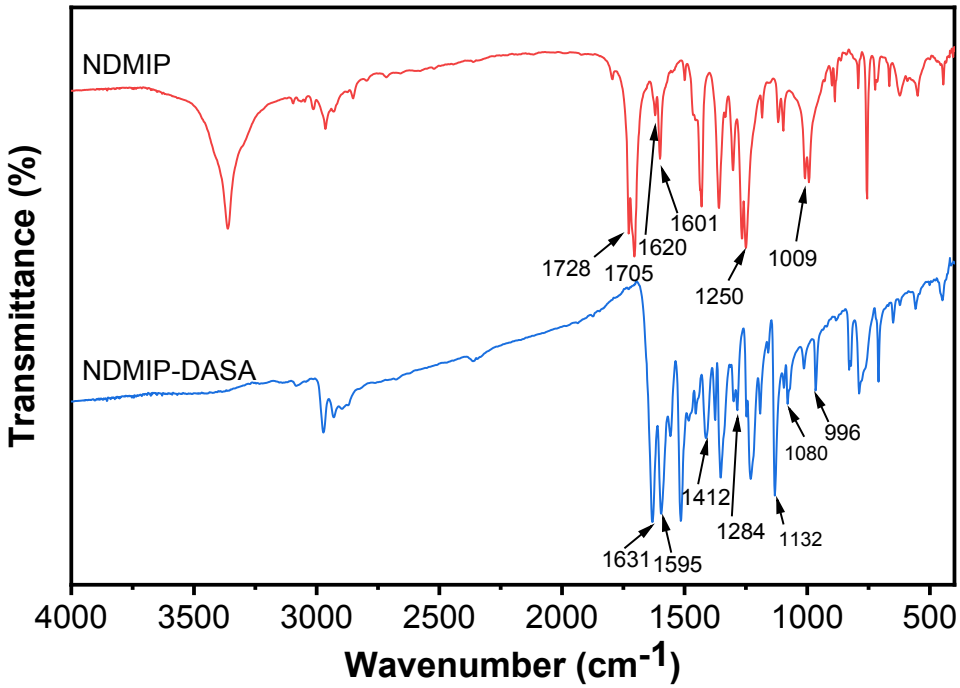


**Figure S2.** FTIR spectra of NDMIP and NDMIP-DASA

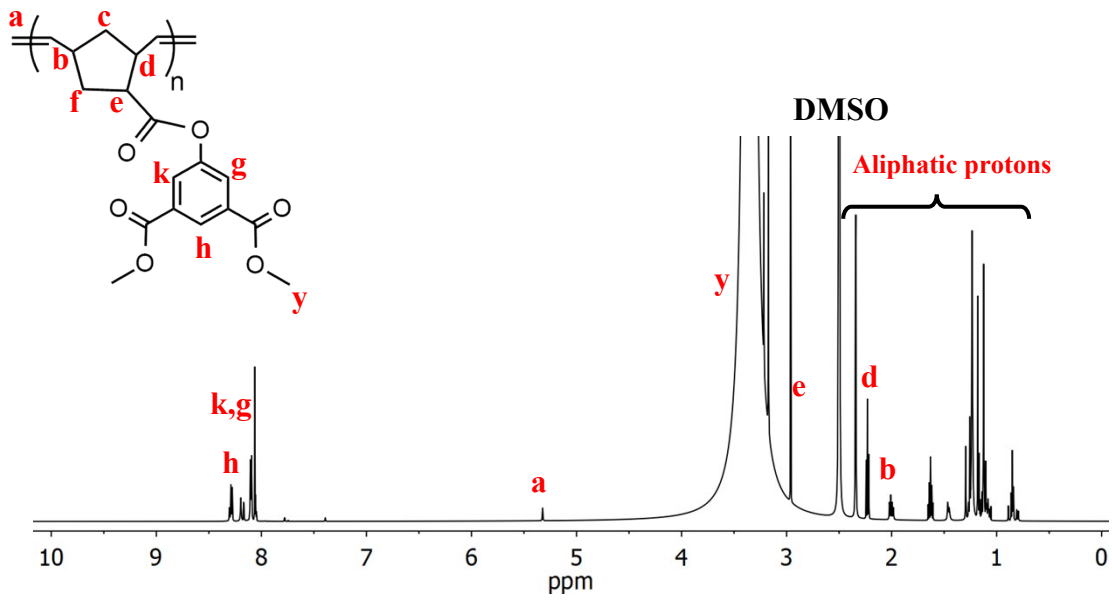


**Figure S3.** $^{1}$H NMR spectra of PNDMIP in DMSO-$d_6$

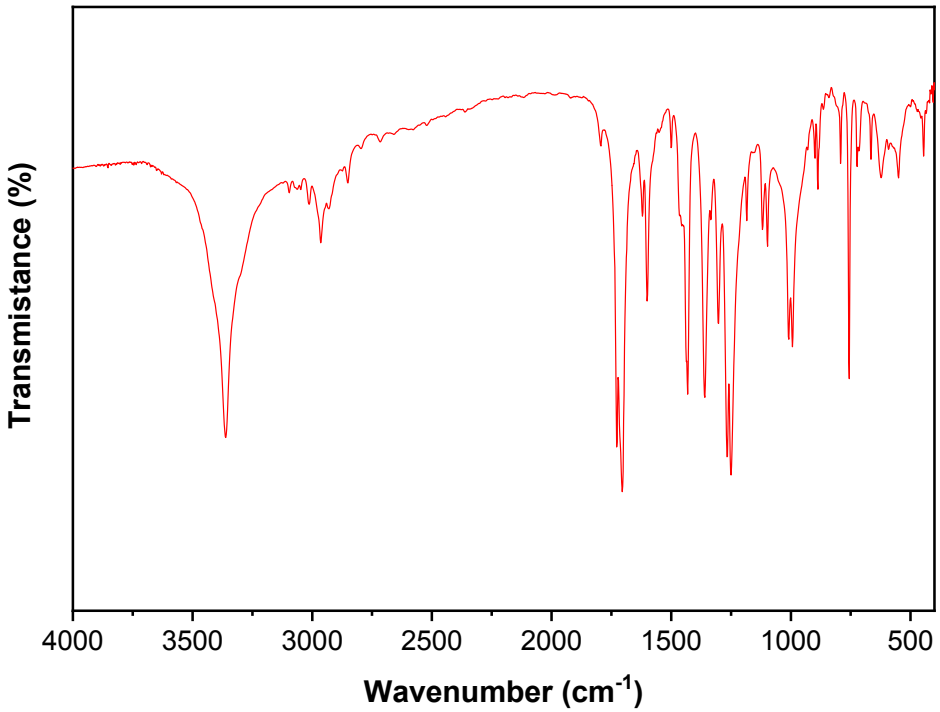


**Figure S4**. FTIR spectra of PNDMIP

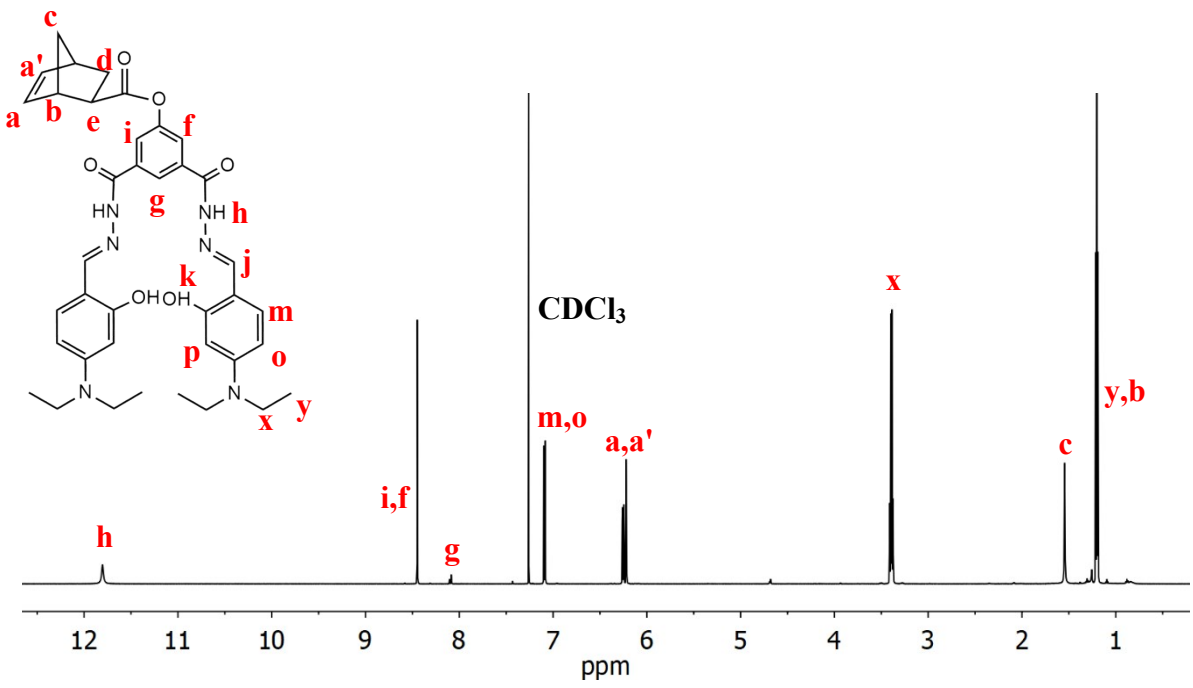


**Figure S5.** $^{1}$H NMR of NDMIP-DASA in $CDCl_3$

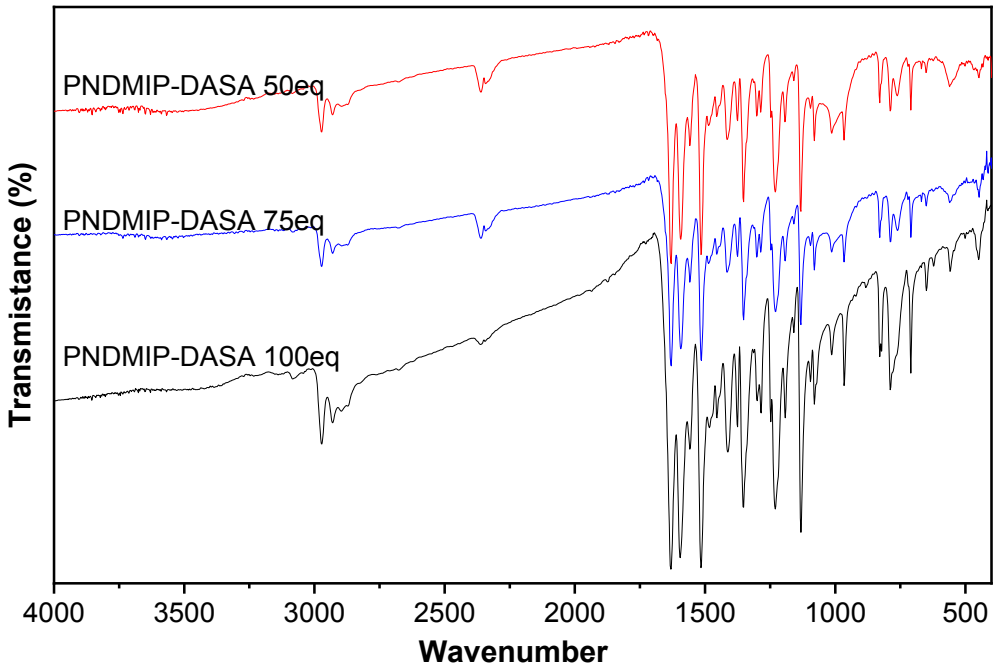


**Figure S6.** FTIR spectra of PNDMIP-DASA 24k, 39k and 56k.

**Table S1.** The benchmark calculations of adsorption maximum for the sensor **M**, which considered different DFT functionals such as B3LYP, CAM-B3LYP, M062X, ωB97XD, and PBE0 with and without THF solvent.

| Basis Set | CAM-B3LYP | CAM-B3LYP (Solv.) | wB97 | wB97 (Solv.) | B3LYP | B3LYP (Solv.) | M062X | M062X (Solv.) | Exp. Value |
|---|---|---|---|---|---|---|---|---|---|
| 6-31G(d) | 319.43 | 326.52 | 294.74 | 300.98 | 403.3 | 408.21 | 321.9 | 329.12 | 422 |

**Table S2.** Table comprising molecular weight and PDI of PNDMIP-DASA by GPC.

| **Homopolymer** | **MW (Da)** | **Polydispersity** |
|---|---|---|
| PNDMIP-DASA 24k | 24039 | 1.04 |
| PNDMIP-DASA 39k | 38964 | 1.02 |
| PNDMIP-DASA 56k | 56549 | 1.13 |

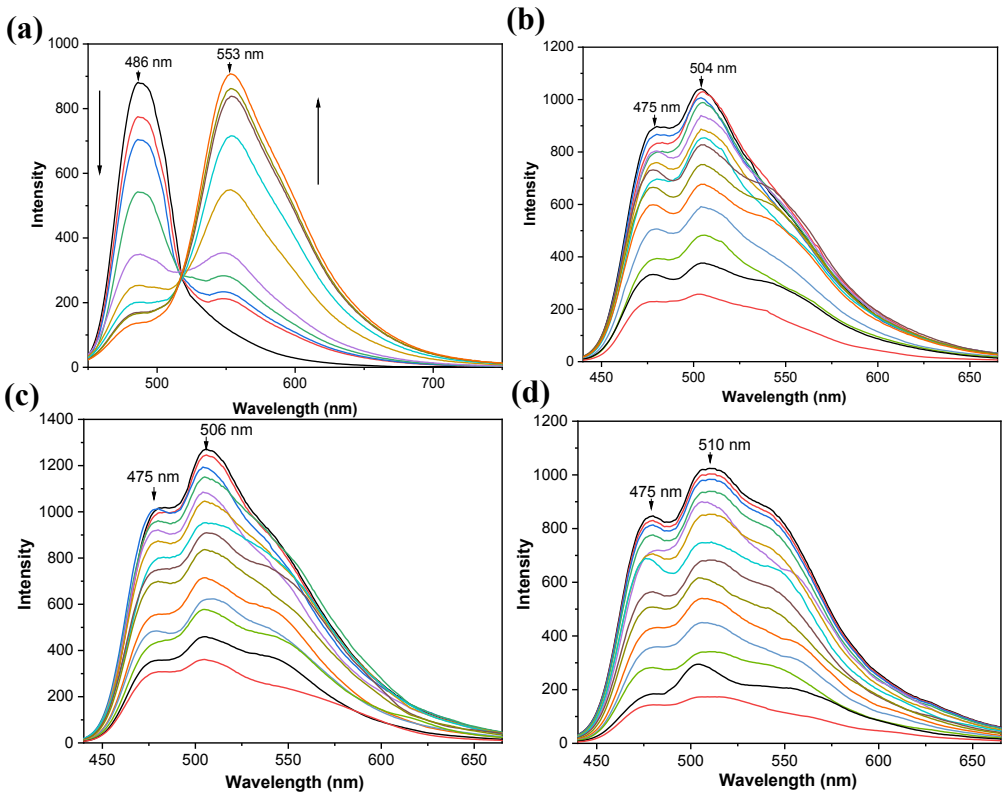


**Figure S7.** Change in fluorescence spectra of NDMIP-DASA (a), PNDMIP-DASA 24k (b), 39k (c), 56k (d) in THF:DIW (2:8) (6.5 ppm) upon gradual addition of $Al^{3+}$ ion.

**Limit of detection (LOD)**

Based on the colorimetric and fluorescence titration, the detection limit (LOD) was calculated using the following equation:

$$LOD = \frac{3\sigma}{k}$$

Where $\sigma$ represents the standard deviation of blank samples, and $k$ represents the slope between the absorption intensity ratio ($A_{511\ nm}/A_{422\ nm}$) or emission intensity versus the $Al^{3+}$ concentration. (*J. Mater. Chem. B*, **2020**; 8(16):3557-3565; *Sens. Actuators B Chem.* **2015**; 208:75-84)

**Table S3.** Limit of detection (LOD) of NDMIP-DASA and PNDMIP-DASA by UV/Vis and fluorescence spectroscopy

| **Sensors** | **LOD by UV/Vis spectroscopy (nM)** | **LOD by fluorescence spectroscopy (nM)** |
|---|---|---|
| NDMIP-DASA | 70.82 | 27.60 |
| PNDMIP-DASA 24k | 56.89 | 16.13 |
| PNDMIP-DASA 39k | 15.69 | 7.44 |
| PNDMIP-DASA 56k | 47.74 | 2.94 |

**Table S4.** The dominant structure parameters of sensor **M** and the complex **M-Al$^{3+}$** in the ground state and excited state (*)

| | Coordination Number | Dihedral angle (°) | | Bond length (Å) | | | |
|---|---|---|---|---|---|---|---|
| | | $D_1$ | $D_2$ | $d_{Al-O1}$ | $d_{Al-O2}$ | $d_{Al-O3}$ | $d_{Al-N}$ |
| M | - | 29.33 | 29.21 | | | | |
| M* | - | 24.71 | 11.71 | | | | |
| M-Al$^{3+}$ | 4 | 0.40 | 0.05 | 1.82 | 1.77 | 1.72 | 1.91 |
| M-Al$^{3+}$* | 4 | 1.90 | 0.16 | 1.81 | 1.77 | 1.72 | 1.92 |

**Table S5**. The dominant structure parameters of sensor **D** and the complex **D-Al$^{3+}$** in the ground state and excited state (*)

| | Coordination Number | Dihedral angle (°) | | | | Bond length (Å ) | | | | | |
|---|---|---|---|---|---|---|---|---|---|---|---|
| | | $D_1$ | $D_2$ | $D_3$ | $D_4$ | $d_{Al\text{-}O1}$ | $d_{Al\text{-}O2}$ | $d_{Al\text{-}O3}$ | $d_{Al\text{-}O4}$ | $d_{Al\text{-}N5}$ | $d_{Al\text{-}N18}$ |
| D | - | 129.77 | 46.84 | -32.2 | -151.50 | | | | | | |
| D* | - | 130.31 | 43.00 | -24.67 | -167.71 | | | | | | |
| D-Al$^{3+}$ | 6 | -6.99 | 150.43 | -151.15 | 153.37 | 1.85 | 1.91 | 1.85 | 2.06 | 1.98 | 2.03 |
| D-Al$^{3+}$* | 6 | -8.7 | 151.16 | -171.1 | 153.42 | 1.91 | 1.84 | 1.97 | 1.87 | 1.99 | 2.04 |

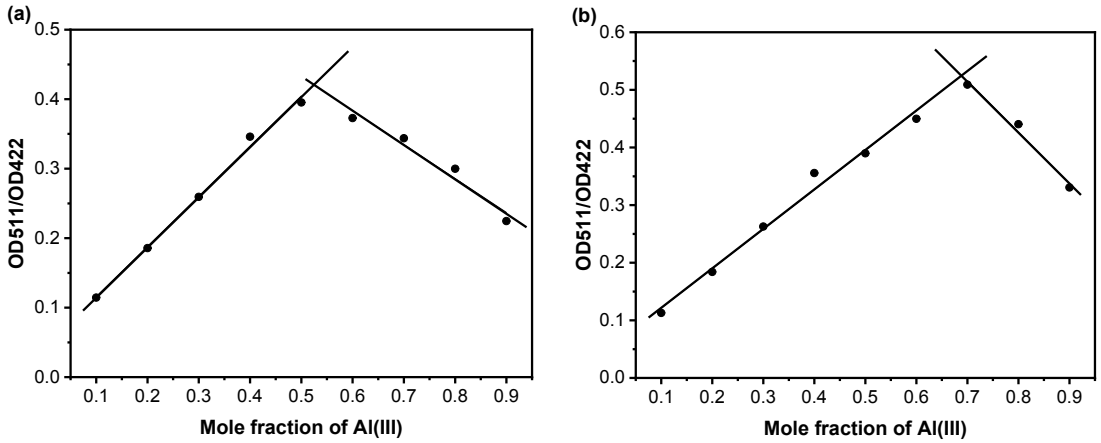


**Figure S8.** Job's plot for stoichiometry of NDMIP-DASA (a) and PNDMIP-DASA (b) with $Al^{3+}$ by UV/Vis spectroscopy.

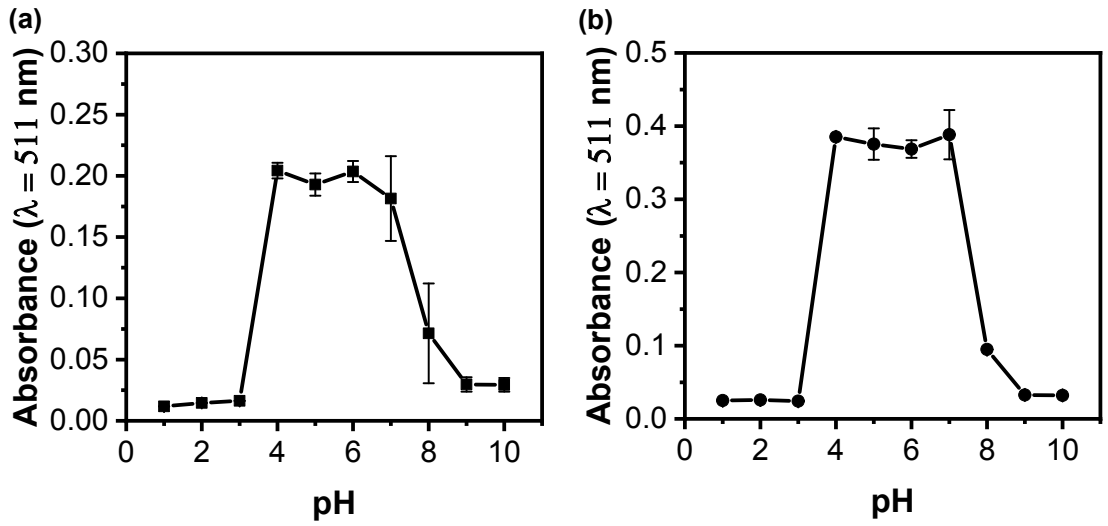


**Figure S9.** The pH effect on absorption (λ = 511 nm) of NDMIP-DASA (a) and PNDMIP-DASA (b) in the presence of $Al^{3+}$ (10 μM).

**Table S6.** Comparison of NDMIP-DASA and PNDMIP-DASA with previous reports on $Al^{3+}$ sensors in literature.

| Type | Probes | Solvent system | Limit of detection (M) | References |
|---|---|---|---|---|
| Polymer probes | PNDMIP-DASA | THF/ Water (2:8, v/v) | $2.94\times10^{-9}$ | This work |
| | PEGSB | Water | $1.32 \times 10^{-8}$ | *Tetrahedron,* **2021,** *79, 131888.* |
| | mPEG-Dye–Biotin | Water | $2.02\times10^{-8}$ | *J. Mater. Chem. B,* **2020**,8, 3557-3565 |
| | PEGBAB | Water | $4.05 \times 10^{-9}$ | *Polymers*, **2019**, 11, 573 |
| | Zn(DMA)(TBA) | Water | $1.97 \times 10^{-6}$ | *Inorg. Chem. Front.,* **2017**,4, 1888-1894 |
| Small molecule probes | NDMIP-DASA | THF/ Water (2:8, v/v) | $2.76\times10^{-8}$ | This work |
| | ZXQ | MeCN/Water (95:5, v/v) | - | *Inorg. Chem. Commun.*, **2020**, 108168 |
| | NDHIPH | HEPES/DMSO | $2.53\times10^{-9}$ | *ACS Omega* **2019**, 4, 18520−18529 |
| | BPD | Britton-Robinson buffer | $2.65 \times 10^{-8}$ | *Sens. Actuators B Chem.* **2019**, *294, 14–23* |
| | A, B and C | ACN/ Water | $1.03\times 10^{-7}$, $3.17\times 10^{-7}$, $9.1\times 10^{-8}$ | *Mater. Chem. Phys.,* **2019**, 233, 89–101 |
| | DFSB | EtOH/ Water | $3.7\times 10^{-8}$ | *RSC Adv.,* **2018**, 8, 31889–31894 |
| | $H_2VM$ | HEPES | $11.34 \times 10^{-9}$ | *Dalton Trans.*, **2018,** 47, 15907–15916 |